International Conference on Nuclear Data for Science and Technology 2007
DOI: 10.1051/ndata:07433

(n,xn) measurements at 96 MeV

I.C. Sagrado García[1,2,a], G. Ban[1], V. Blideanu[2], J.M. Fontbonne[1], G. Iltis[1], F.R. Lecolley[1], J.F. Lecolley[1], J.L. Lecouey[1], T. Lefort[1], N. Marie[1], J.C. Steckmeyer[1], C. Le Brun[3], J. Blomgren[4], C. Johansson[4], J. Klug[4], A. Öhrn[4], P. Mermod[4], N. Olsson[4], S. Pomp[4], M. Österlund[4], U. Tippawan[4,5], A.V. Prokofiev[6], P. Nadel-Turonski[7], M. Fallot[8], Y. Foucher[8], A. Guertin[8], F. Haddad[8], and M. Vatré[8]

[1] LPC Caen-Université de Caen, CNRS/IN2P3, ENSICAEN, 6 bd du Maréchal Juin, 14050 Caen Cedex 04, France
[2] CEA-Saclay DSM/DAPNIA/SENAC, Gif-sur-Yvette, France
[3] LPSC, Grenoble, France
[4] Department of Neutron Research, Uppsala University, Sweden
[5] Fast Neutron Research Facility, Chiang Mai University, Thailand
[6] The Svedberg Laboratory, Uppsala University, Sweden
[7] George Washington University, Washington, DC, USA
[8] SUBATECH, Nantes, France

Abstract. Double differential cross section for neutron production were measured in 96 MeV neutrons induced reactions at the TSL laboratory in Uppsala (Sweden). Measurements for Fe and Pb targets were performed using simultaneously two independent setups: DECOI-DEMON and CLODIA-SCANDAL. The double differential cross section were measured for an angular range between 15 and 100 degrees and with low-energy thresholds (1–2 MeV). Elastic distribution, angular distribution, energy distribution and total inelastic cross section were derived from measured double differential cross section. Results are compared with predictions given by several simulation codes and with other experimental data.

1 Introduction

Future Accelerator-Driven Systems (ADS) will couple a high-energy intense proton beam (~1 GeV and a few mA) with a spallation target made of heavy elements and a sub-critical reactor core. The proton beam impinging on the ADS target will yield a large amount of spallation products, mainly neutrons, protons and light charged particles, with energies ranging from some MeV to the GeV region.

Under 20 MeV the nuclear data libraries are nearly complete [1]. Above 200 MeV the cross section predictions by Intra Nuclear Cascade (INC) models are in good agreement with the experimental data [2–4]. However for energies from 20 to 200 MeV there are very few high-quality data, particularly for (n,xn) inelastic measurements [5].

In the framework of the European research program EUROTRANS-NUDATRA [6], measurements on (n,xn) double differential cross section using lead and iron targets for an incident neutron beam at 96 MeV were carried out at the Svedberg Laboratory, Uppsala (Sweden). The measurements were accomplished using two different setups: CLODIA-SCANDAL (fig. 1) and DECOI-DEMON (fig. 2). The double differential cross section were obtained for an angular range between 15 and 100 degrees and with low-energy thresholds (1–2MeV). Elastic distribution, angular distribution, energy distribution and total inelastic cross section were obtained from measured double differential cross section. Comparisons with the existing data and with theoretical model calculations are discussed.

[a] Presenting author,
e-mail: inmaculada.sagradogarcia@cea.fr

2 Experimental setup

To measure the high-energy part of the neutron spectrum, above 40 MeV, a new setup labelled CLODIA (Chamber for LOcalization with DrIft and Amplification) was constructed for the measurement of the high-energy part of the neutron energy spectrum. CLODIA consists of seven (n,p) converters and eight multidrift chambers to measure the recoil proton trajectories and determine in which converter the neutron interaction took place. In addition, one SCANDAL arm was used to measure the proton residual energy. Neutron energy is derived from the angle of the well-known backward elastic neutron-proton scattering and from the energy of the recoiling proton.

To measure the low-energy part of the neutron spectrum, below 50 MeV, a time-of-flight telescope labelled DECOI-DEMON was developped at the LPC Caen laboratory. DECOI is a neutron-to-proton converter made of a plastic scintillator brick (NE102, $5 \times 9 \times 15\,\mathrm{cm}^3$). DEMON is a neutron detector made of a cylindrical liquid scintillator (NE213 with a 16 cm diameter and a 20 cm thickness). In front of a DEMON cell, a 5 mm thick plastic scintillator was added for charged particle rejection. Incoming neutron, weakly deflected in DECOI, is detected and identified using DEMON; its energy is measured by the well-known time-of-flight technique.

Two different experiments were performed using the neutron beam available at the TSL laboratory in Uppsala (Sweden). Between the feasibility test realized in 2003 and the measurements realized in 2004, the Uppsala neutron facility has been modified in order to increase the neutron flux, from 10^5 to 10^6. Description of both facilities are given in the refs. [9] and [10]. Neutrons are produced by ^{7}Li(p, n)^{7}Be reactions using a 100 MeV proton beam impinging on a lithium target.

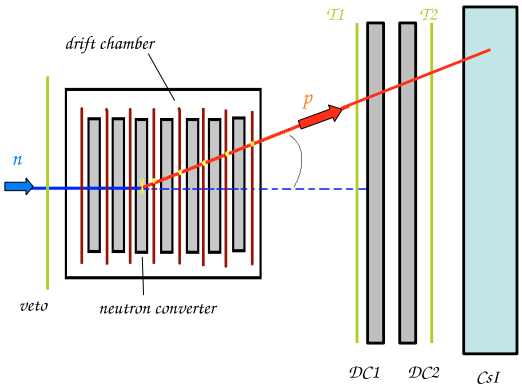

Fig. 1. Schematic view of the CLODIA-SCANDAL setup.

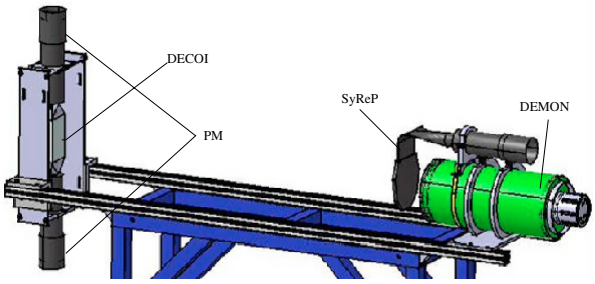

Fig. 2. Schematic view of the DECOI-DEMON setup.

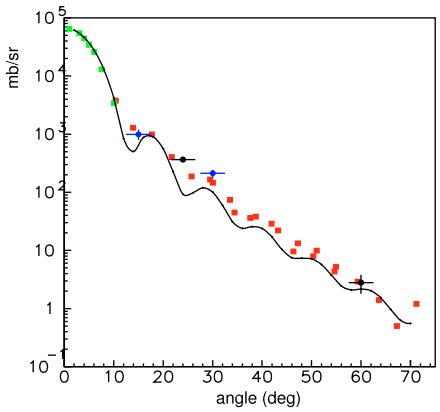

Fig. 3. Elastic cross section Pb(n,n) obtained with CLODIA-SCANDAL and DECOI-DEMON (circles) compared to experimental data from [11] and [12] (squares), and to optical model calculations [13] (solid line).

Produced neutrons are separated from the primary proton beam using a magnetic deflection. The neutron beam is collimated before its arrival at the experimental hall. About 50% of neutrons are in a 96 MeV peak and the rest in low energy tail. The beam monitoring is provided by a Faraday cup where the proton beam is dumped and by a fission detector composed of thin-film breakdown counters placed in the experimental hall.

3 Results

Double differential distributions for $T_n > 40$ MeV were obtained using CLODIA-SCANDAL setup. Distributions for $T_n < 50$ MeV were obtained using the DECOI-DEMON

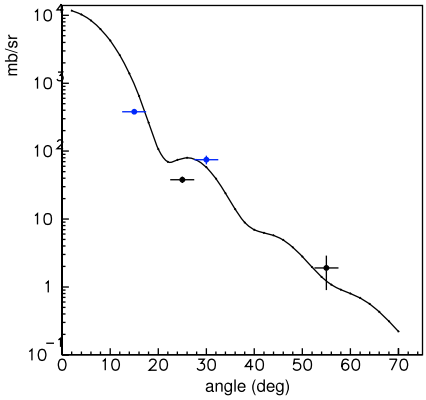

Fig. 4. Elastic cross section Fe(n,n) obtained with CLODIA-SCANDAL and DECOI-DEMON (circles) compared to optical model calculations [13] (solid line).

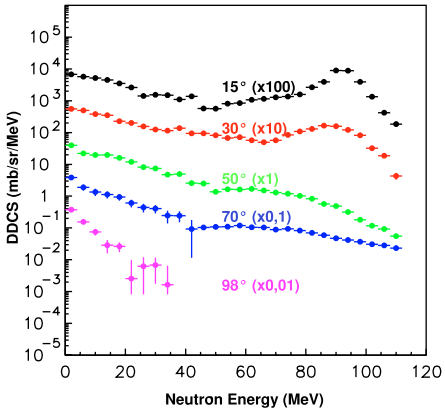

Fig. 5. Double differential cross section Pb(n,xn).

setup. In the overlap energy region, from 40 to 50 MeV, the two set of measurement differs from less than 10%.

For small angles an elastic peak centered at 96 MeV (energy beam) is clearly observed. Elastic cross section were calculated via direct integration of this elastic peak. DECOI-DEMON device also allows the elastic cross section measurements (more details can be found in [7,8]). The obtained results are in good agreement with existing experimental data [11,12] and with optical model calculations [13] (figs. 3 and 4). This agreement validates the cross section normalization procedure.

Figures 5 and 6 show the complete double differential distributions for lead and iron target for an angular range from 15 to 100 degrees and with an energy threshold of 1–2 MeV. Energy distributions were obtained from measured double differential cross section using the Kalbach parameterization [14,15]. Total inelastic cross section were calculated from energy distribution integration in the measured energy region (table 1).

4 Model and experimental data comparison

Energy differential distributions for lead and iron were calculated using several available models: GNASH [16] and INCL4-ABLA [17,18] in MCNPX [19], FLUKA and

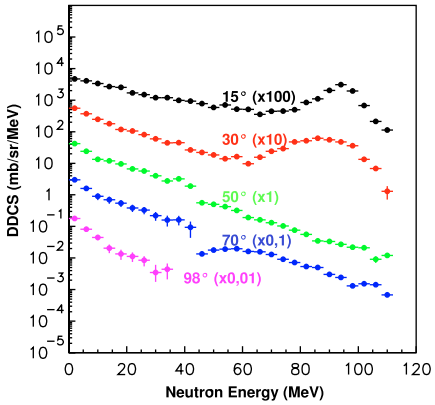

Fig. 6. Double differential cross section Fe(n,xn).

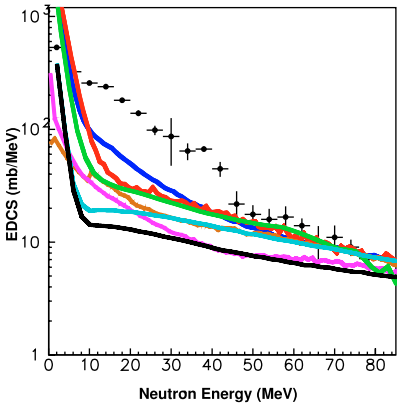

Fig. 7. Energy differential cross section Pb(n,xn) derived from double differential cross section using the Kalbach systematic (points) compared to theoretical prediction (lines): MCNPX/GNASH (dark blue), MCNPX/INCL4-ABLA (red), GEANT3/FLUKA (brown), GEANT/GHEISHA (pink), TALYS (green), DYWAN (black) and DYWAN+symmetry energy term (blue).

GHEISA in GEANT3 [20], TALYS [21], and the microscopic model DYWAN [22,23] with and without a symmetry energy term. Comparison between those calculations and the experimental data are shown in figures 7 and 8. We observe a systematic data under-estimation.

Total neutron production were calculated by direct integration of the measured energy region for the two MCNPX calculations (table 1). For the iron target, the disagreement is clear and total neutron production are underestimated by a factor of three. The better agreement found for the lead target is due to a compensating effect between evaporation and pre-equilibrium emission in MCNPX calculations.

We have also made the comparison between the data given in this work and the available (n,xn) data [24] for

Table 1. Total neutron production (in mb) calculated in the measured energy region.

target	GNASH	INCL4/ABLA	DATA
Fe	1459	1577	4304
Pb	5011	5964	6132

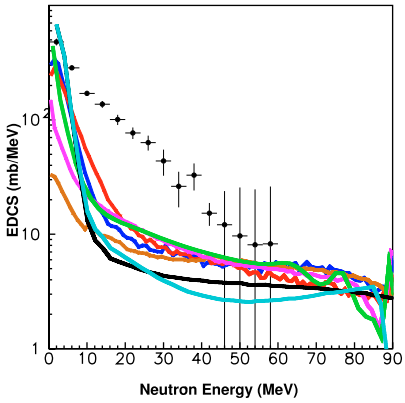

Fig. 8. Energy differential cross section Fe(n,xn)derived from double differential cross section using the Kalbach systematic (points) compared to theoretical prediction (lines): MCNPX/GNASH (dark blue), MCNPX/INCL4-ABLA (red), GEANT3/FLUKA (brown), GEANT/GHEISHA (pink), TALYS (green), DYWAN (black) and DYWAN+symmetry energy term (blue).

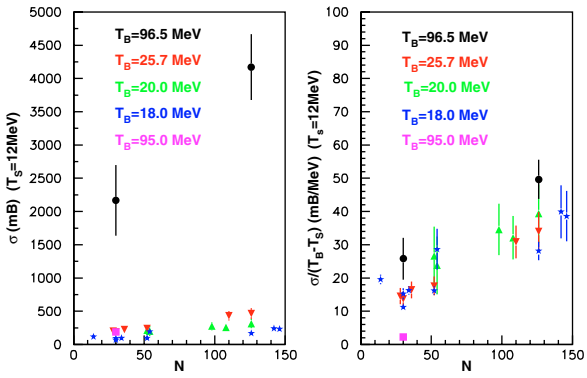

Fig. 9. Pre-equilibrium cross section obtained from the available existing data (symbols) and from the present work (black circles) represented as a function of the number of neutron of the target element.

different targets. For each experimental data set (included ours) pre-equilibrium cross section was calculated by integration of the energy distribution with an energy threshold of $T_{\text{threshold}} = 12$ MeV. Results presented as a function of the number of neutron in the target element are shown in figure 9 (left panel) and we can see that our results are far from the others. Nevertheless one have to consider the fact that all available (n,xn) data except one were obtained at neutron beam energy lower than 30 MeV. In order to obtain an information not dependant of the incident beam energy, pre-equilibrium cross section were divided by the quantity $(T_{beam} - T_{threshold})$. Results are presented in the figure 9 (right panel). A good agreement between the different experimental data and the results obtained in this work is found.

5 Summary

Double differential cross section for neutron production were measured in 96 MeV neutrons induced reactions on lead and iron targets. Measurements were obtained for an angular range between 15 and 98 degrees and with an energy threshold of

1–2 MeV. The elastic cross section measured are in good agreement with available experimental data and with optical model calculation; this agreement gives us confidence in the cross section normalization procedure.

Energy distributions were obtained from measured double differential cross sections using the Kalbach systematic. Total inelastic cross sections were also derived via energy distribution integration. Comparison with several theoretical predictions (MCNPX, GEANT, TALYS, DYWAN) shows a systematic model underestimation in particular in the 10 to 50 MeV energy range. Comparison with available experimental data (EXFOR Data Bank) exhibits a general trend in which all data are included when taking into account pre-equilibrium cross section over $(T_{beam} - T_{threshold})$.

The authors wish to dedicate this contribution to their recently deceased colleague and friend Gilles Iltis, whose contributions to the work presented here and elsewhere were vital.

References

1. HINDAS, High and Intermediate energy Nuclear Data for Accelerator-Driven Systems, European Community, contract No. FIKW-CT-2000-0031.
2. H.W. Bertini, Phys. Rev. (1969), p. 188.
3. A. Boudard, J. Cugnon, S. Leray, C. Volant, Phys. Rev. C **66**, 044615 (2002).
4. H. Kumawat, V.S. Barashenkov, Eur. Phys. J. A **26**, 61 (2005).
5. E.L. Hjort et al., Phys. Rev. C **53**, 237 (1996).
6. EUROTRANS-NUDATRA, EUROpean research program for the TRANSmutation of high level nuclear waste in an Accelerator Driven System, contract No. FI6W-CT-2004-516520.
7. I. Sagrado Garcia, *Mesure des sections efficaces (n,xn) 96 MeV*, Université de Caen, Ph.D. thesis.
8. G. Ban et al., *Neutron emission spectrum measurements in the 1-100 MeV energy range* (submitted to Nucl. Instrum. Meth. A).
9. H. Cond et al., Nucl. Instrum. Meth. A **292**, 121 (1990).
10. S. Pomp et al., *International Conference on Nuclear Data for Science and Technology, Santa Fe, 2004*.
11. G.L. Salmon, Nucl. Phys. **21**, 15 (1960).
12. J. Klug et al., Phys. Rev. C **68**, 064605 (2003).
13. A.J. Koning, J.P. Delaroche, Nucl. Phys. A **713**, 231 (2003).
14. C. Kalbach, Phys. Rev. C **23**, 112 (1981).
15. C. Kalbach, Phys. Rev. C **37**, 2350 (1988).
16. M.B. Chadwick et al., *Cross Section Evaluations to 150 MeV for ADS and Implementation in MCNP* (1999).
17. A. Boudard et al., Phys. Rev. C **66**, 044615 (2002).
18. A.R. Junghans et al., Nucl. Phys. A **629**, 635 (1998).
19. D.B. Pelowitzet et al., *MCNPX User's Manual 2.5.0*, Los Alamos National Laboratory (2004).
20. GEANT Detector Description and Simulation, CERN Program Library.
21. *TALYS 0.64*, A.J. Koning, S. Hilaire, M. Duijvestijn, NRG Report 21297/04.62741/P FAI/AK/AK (2004).
22. B. Jouault, F. Sbille, V. de la Mota, Nucl. Phys. A **628**, 119 (1998).
23. V. de la Mota, F. Sbille, Eur. Phys. J. A **12**, 479 (2001).
24. EXFOR Data Bank, Nuclear Energy Agency, http://www.nea.fr/.